Cell Proliferation

Cell Prolif., 2014, **47**, 81–90 doi: 10.1111/cpr.12083

Inhibition of osteogenic differentiation of mesenchymal stem cells by copper supplementation

S. Li*, M. Wang*, X. Chen†, S-F. Li‡, J. Li-Ling§,¶ and H-Q. Xie*,†

**Laboratory of Stem Cell and Tissue Engineering, Regenerative Medicine Research Center, West China Hospital, Sichuan University, Chengdu, 610041, China, †Laboratory of Stem Cell and Tissue Engineering, State Key Laboratory of Biotherapy, Sichuan University, Chengdu, 610041, China, ‡Key Laboratory of Transplant Engineering and Immunology of Ministry of Health, West China Hospital, Sichuan University, Chengdu, 610041, China, §Laboratory of Disease Genomics and Bioinformatics, State Key Laboratory of Biotherapy, Sichuan University, Chengdu, 610041, China and ¶Sino-Dutch Biomedical and Information Engineering School, Northeastern University, Shenyang, 110819, China*

Received 25 July 2013; revision accepted 21 September 2013

Abstract

Objectives: Copper has been added to scaffolds when investigating bone repair, as an agent to promote vascularization; however, little is known concerning its effect on mesenchymal stem cells (MSCs), which are considered to be the origin of osteoblasts. In this study, we have aimed to elucidate effects of copper on osteogenic differentiation of MSCs.

Materials and methods: Rat bone marrow MSCs (rBMSCs) were used as a model. Their viability was assessed by MTT assay and Roche's CASY cell counter test and calcium deposition was evaluated by staining with alizarin red S. Fluorescent phalloidin F-actin stain was used to evaluate cytoskeletal changes, protein expressions were investigated by western blotting and mRNA levels were analysed using Q-PCR. A rat model for ectopic bone formation was used to assess effects of copper on MSCs *in vivo*.

Results: Copper supplementation resulted in inhibition of osteogenesis of rBMSCs, along with reduction in expression of a number of osteogenic genes, alkaline phosphatase activity and formation of bone nodules. Cytoskeletal changes to cells during osteogenesis was inhibited by copper supplementation. *In vivo* study confirmed that copper could inhibit collagen formation whilst promoting angiogenesis.

Conclusions: Our study demonstrated that copper inhibited osteogenic differentiation of rBMSCs *in vitro*. The findings caution appropriate use of copper and have laid a foundation for further research.

Correspondence: H-Q. Xie, Laboratory of Stem Cell and Tissue Engineering, Regenerative Medicine Research Center, West China Hospital, Sichuan University, Chengdu 610041, China. Tel.: +86 28 85164088; Fax: +86 28 85164088; E-mail: xiehuiqi@scu.edu.cn

Introduction

The importance of angiogenesis in skeletal formation and bone repair has been noticed for around 300 years (1,2). During bone formation, homeostasis of osteoblasts, osteoclasts, endothelial cells, angiogenic factors and their interactions is crucial. Promotion of angiogenesis has been shown to be critical for skeletal development and repair of bone fractures (3,4), and has also been proposed as a new therapeutic strategy for bone regeneration (5,6).

Promotion of angiogenesis and stimulation of endothelial cell proliferation by copper (Cu) have been appreciated for a number of decades (7) and copper has been used clinically as a therapeutic agent to promote vascularization (8–10); in this capacity it has also been added to scaffolds during bone repair (11,12).

Mesenchymal stem cells (MSCs) (having the capacity for self-renewal and differentiational multipotency), have been used as seed cells for bone tissue engineering, being considered to be the origin of osteoblasts (13,14). Thus, delineating effects of copper on MSC osteogenesis has important implications for bone tissue repair and the appropriate use of copper as an agent for promoting angiogenesis.

Numbers of investigations have assessed effects of copper on osteogenic differentiation of MSCs (15,16). However, it is worth noting that in most cases, concentration of copper (ranging between 50 and 500 μmol/l) has been much greater than its normal physiological levels. In previous studies by our group, we have demonstrated that copper at physiological levels can stimulate population growth of endothelial cells derived from the

human umbilical vein, which was eNOS-dependent (17). We have also derived a copper concentration of 5 μmol/l in cultures from which could be achieved in blood of mice on a dietary supplement of 20 mg/kg (18) copper; this was verified by *in vitro* experimentation (17). It is thus critical to determine effects of copper on MSC differentiation at physiological copper levels, so that *in vitro* studies can be extrapolated to *in vivo* conditions, and provide valuable information prior to animal study.

Several factors are known to be involved in regulation of osteogenic differentiation of MSCs. *Runx2* is a regulator required for expression of further downstream genes (19,20). High levels of copper can stabilize HIF-1α, which in turn can lead to its accumulation and enhanced HIF transcriptional activity (21,22). Hypoxia can suppress osteogenesis of human MSCs by regulation of *Runx2* through TWIST (23). Here, we have explored whether copper could regulate rat bone marrow MSC (rBMSC) osteogenesis *via* the *Runx2*-related pathway. We have also aimed to verify any such effects using a rat model, for ectopic bone formation.

Materials and methods

Sprague–Dawley (SD) rats were purchased from the Laboratory Animal Academy of Sichuan Medical Sciences Institute (License Number SCXK2004-15). The rats were kept in cages under standard laboratory conditions and given rat chow and allowed free access to water.

Ethical statement

All experimental procedures were approved by Sichuan University Animal Care and Use Committee in accordance with the Principles of Laboratory Animal Care formulated by the National Society for Medical Research.

Cell culture and treatment

Rat bone marrow MSCs were harvested from the 4- to 7-day-old SD rats. Using a previously described method (24), after carefully removing skin and muscle, whole bone marrow was flushed from tibial and femoral bones using a 1-ml syringe containing Dulbecco's modified Eagle's medium-low glucose (DMEM-L) (Gibco, New York, NY, USA) supplemented with 10% foetal bovine serum (FBS) (Gibco, Mulgrave, VIC, Australia) and 1% antibiotic- antimycotic (Gibco, New York, NY, USA). Tissues were plated into 25 cm^2 flasks and incubated in 5% CO_2 at 37 °C. Medium was replaced the following day and refreshed every 2–3 days. When cell colonies grew to 80–90% confluence, cells were washed twice in phosphate-buffered saline (PBS) and treated with 0.25% trypsin (Sigma, St Louis, MO, USA) in 1 mM EDTA (Sigma). They were then resuspended in serum-supplemented medium, counted, and plated to 5–7 × 10^5 cells/25 cm^2 flask, and incubated in 5% CO_2 at 37 °C. rBMSCs from the third passage were seeded into 3.5 mm dishes at 20 000 cells/dish in 2 ml DMEM-L supplemented with 10% FBS. On the following day, dishes were divided into 4 groups: (i) Control, cultured in Dulbecco's modified Eagle's medium-high glucose (DMEM-H) (Gibco) supplemented with 10% FBS; (ii) Cu group, cultured in DMEM-H supplemented with 10% FBS and 5 μmol/l $CuSO_4$ (Kelong, Chengdu, China); (iii) Osteo group, cultured in osteogenic differentiation inducing medium, that is, DMEM-H supplemented with 10% FBS, 100 nM dexamethasone (Sigma), 10 mM β-glycerophosphate (Sigma), 50 μg/ml ascorbic acid (Sigma) and 10% FBS; (iv) Osteo+Cu group, cultured in the above osteogenic differentiation inducing medium supplemented with 5 μmol/l $CuSO_4$. Thereafter, cells in each group were incubated for periods of time as indicated. Cultured cells were counted with the aid of a haemocytometer.

Flow cytometry

To analyse cell surface markers, rBMSCs were treated with 0.25% trypsin and 1 mM EDTA, and incubated with fluorescein isothiocyanate (FITC)-conjugated monoclonal antibodies against rat CD29, CD34, CD45 and CD90 (Biolegend, San Diego, CA, USA). Markers expressed on the cells were characterized using flow cytometry (Becton, Dickinson and Company, Franklin Lakes, NJ, USA).

MTT assay

Cells were seeded into 96-well plates at 5000 cells/well in 0.2 ml DMEM-L supplemented with 10% FBS. Viability was determined using colorimetric 3-(4,5-dimethylthiazol-2-yl)-2, 5-diphenyltetrazolium bromide (MTT, Amresco, OH, USA) assay. In brief, cultured cells were washed in PBS. Following replacement with fresh media, 20 μl MTT solution (5 mg/ml) was added. After further incubation for 3.5 h, MTT solution was carefully removed from each well, and MTT formazan crystals were dissolved in 100 μl DMSO (Kelong). Absorbance at 490 nm was measured by spectrophotometry (Spectra Max190; Molecular Devices, Sunnyvale, CA, USA).

Cell viability and size measurement

After exposure to various media for 48 h, cells were washed twice in PBS and treated with 0.25% trypsin in

1 mM EDTA. Subsequently, they were fully dispersed and tested using Roche's CASY cell counter (Roche, Basel, Switzerland).

Alizarin red S staining

After 21 days culture, cells were fixed in 75% ethanol for 15 min. at room temperature and rinsed 3 times in PBS. They were then stained with 0.1% alizarin red S (Sigma) for 30 min. at 37 °C. After 3 washes, dishes were air dried. Photomicrographs were taken using an inverted phase-contrast microscope (Nikon, Tokyo, Japan).

Phalloidin staining

Phalloidin was used to label F-actin to demonstrate cytoskeletal changes. After 5 days culture, cells were fixed in 4% formalin for 20 min. at room temperature, washed 3 times in PBS and stained in 5 μg/ml fluorescent phalloidin conjugate solution (Phalloidin-FITC; Life Technologies, Carlsbad, CA, USA) in PBS for 40 min at 37 °C. They were then washed several times in PBS to remove unbound phalloidin conjugate. Photomicrographs were taken using a confocal laser scanning microscope (Nikon).

Histochemical assays of ALP (Kaplow assay)

After 7 days culture, cells were washed in PBS, dried at room temperature for 30 min and incubated in alkaline phosphatase (ALP) medium (0.04% $NaNO_2$, 0.08% basic fuchsin, 10 mg naphthol AS-BI phosphate, 0.5 ml *N,N*-Dimethylformamide) for 2 h at 37 °C. They were then counterstained with methyl green for 10 min. Photomicrographs were taken using an inverted phase-contrast microscope (Nikon).

Q-PCR

Total RNA was extracted from cells harvested after specified treatments using an RNAiso Plus kit (Takara, Shiga, Japan). Complementary DNAs were synthesized with a SYBR PrimeScript™ RT reagent kit (Takara) under the following conditions: denaturation at 95 °C (30 s); 40 cycles at 95 °C (5 s) and 60 °C (20 s) in a IQ5 Multicolor Real-Time PCR Detection System (Bio-Rad, Benicia, CA, USA). Amount of complementary DNA corresponding to 100 ng RNA was amplified using a SsoAdancedTMSYBR Green Supermix Kit (Bio-Rad) with primers for rat glyceraldehyde-3-phosphate dehydrogenase (*Gapdh*), Runt-related transcription factor 2 (*Runx2*), osterix (*Osx*), alkaline phosphatase (*Alp*), bone morphogenetic protein 2 (*Bmp2*), osteocalcin (*Ocn*), osteopontin (*Opn*), peroxisome proliferator activated receptor gamma 2 (*Pparγ2*), collagen type I (*ColI*) and collagen type III (*ColIII*) (Life Technologies). Oligonucleotide primer sequences for the above genes are listed in Table S1. IQ5 software (Bio-Rad) was used to analyse fluorescence data to obtain cycle threshold values. To normalize the data, *Gapdh* was used as internal reference for each reaction. Relative expression was calculated using the $2^{-\Delta\Delta Ct}$ method. All data were expressed as fold-changes.

Protein extraction and western blotting analysis

Cells were rinsed in PBS and lysed with RNAiso Plu (Takara). Protein concentrations were determined with a *DC*™ Protein Assay (Bio-Rad). After boiling for 5 min in sample loading buffer, aliquots of cell lysates were run on 12% SDS polyacrylamide gel. Proteins were transferred to PVDF membrane filters, which were then blocked for 1 h with TBS containing 5% non-fat dry milk and 0.05% Tween-20, and incubated overnight at 4 °C with the primary antibodies. Filters were washed 3 times for 10 min. each with TBS. After incubating for 1 h in secondary antibodies Anti rat Runx2 (ab133580) (Abcam, Cambridge, UK), PPARγ2 (ab45278) (Abcam), OCN (ab13420) (Abcam) and GAPDH (sc25778) (Santa Cruz Biotech, CA, USA), filters were washed and developed using Immobilon Western Chemiluminescent HRP Substrate (Millipore, Billerica, MA, USA). Densitometric analysis was carried out using Quantity One software (Bio-Rad).

Ectopic bone formation

Using DMEM-H as solvent, alginic acid sodium salt (ALG) (Sigma) was used to prepare gel containing 4% sodium alginate. rBMSCs from the third passage were mixed with prepared gel and adjusted to 1×10^5 cells/ml. $CuSO_4$ was added to prepared alginate gel at final concentration of 5 μM. After thorough mixing, 5% calcium gluconate (Sigma) 100:1 ratio, was added for cross-linking, for 30 s. Demineralized human bone matrix (DBM) (Datsing, Beijing, China) was soaked in cross-linked gel until it was completely filled and DBM/ALG/rBMSCs implants were ready for use.

Rat model

Adult female SD rats, average weight 150–200 g were used to construct the model. All surgical procedures were carried out under intraperitoneal anaesthesia induced by chloral hydrate (0.35 g/kg). For intramuscular

implantation, lumbar regions were shaved and disinfected with iodine. Two incisions were made approximately 0.5–1 cm away from the spine. Lumbar muscles were separated to create an intramuscular space, into which DBM/ALG/rBMSCs biomaterials were implanted. Each animal received 4 implants including two DBM/ALG/rBMSCs implants for control and two DBM/ALG/rBMSCs implants supplemented with 5 μM $CuSO_4$ (n = 5) (Fig. S1). After implantation, wound and skin flaps were immediately closed in two layers using resorbable sutures. Following surgery, animals were allowed free access to food and water and were monitored daily for potential complications or abnormal behaviour. Respectively, at 2 weeks and 2 months after the surgery, animals were sacrificed by injection of lethal doses of chloral hydrate. Histological analysis was subsequently carried out.

Statistical analysis

Data were obtained from 3 independent experiments, expressed as mean ± SEM. One-way ANOVA was used to compare data between Q-PCR experiment groups and differences between groups were estimated by least significant difference test. Data of MTT assay and cell viability and size measurement experiment groups were determined using Student's t-test. Level of significance was considered when $P < 0.05$.

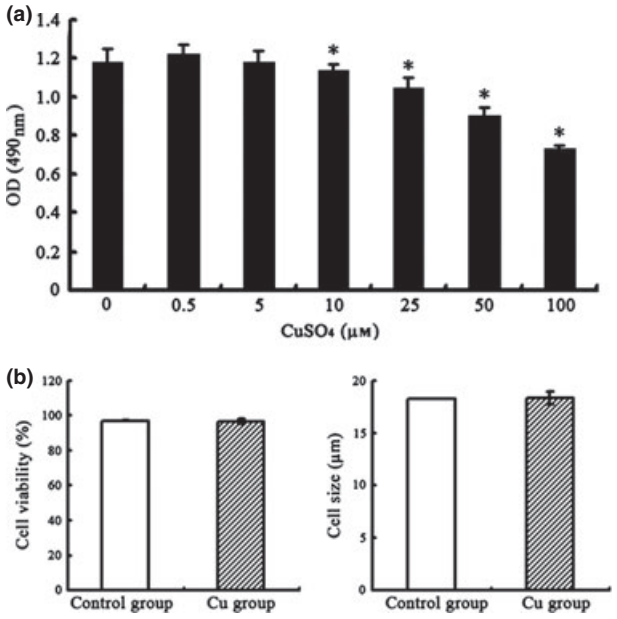

Figure 1. Effect of various concentrations of Cu on rBMSCs. Rat bone marrow mesenchymal stem cells (rBMSCs) were cultured with various concentrations of $CuSO_4$ for 48 h, and their viability was measured by a MTT assay (a). For viability and cell size analysis, rBMSCs were cultured in the presence or absence of 5 μmol/l $CuSO_4$ for 48 h before collection (b). All data were derived from three independent experiments. Each experiment consisted of triplicate samples for a treatment. Values are presented as mean ± SEM. *Significantly different from the control group ($P < 0.05$).

Results

In vitro *culture and characterization of rBMSCs*

To characterize surface markers of third passage rBMSCs, flow cytometric analysis was carried out on cultured cells. As discovered, more than 95% were positive for expression of CD29 and CD90, whilst fewer than 2% expressed detectable levels of CD34 and CD45. As confirmed by a series of staining procedures (alizarin red for mineralized matrix, oil red O for lipid droplets of adipocytes and toluidine blue for methachromatic matrix of cartilage), the rBMSCs readily differentiated into bone, cartilage and fat cells (Fig. S2).

Physiological concentrations of copper suitable to rBMSCs

To determine the range of physiological concentrations of copper for experimental conditions, rBMSCs were exposed to various concentrations of $CuSO_4$ (0, 0.5, 5, 10, 25, 50 and 100 μmol/l) for a total of 48 h. As shown by MTT assay (Fig. 1a), copper supplementation had no significant impact at concentrations between 0 and 5 μmol/l, but had cytotoxic effects at concentrations above 10 μmol/l. Cell viability and size were measured using Roche's CASY cell counter. As shown in Fig. 1b, when treated with 5 μmol/l $CuSO_4$, cells showed no significant difference in size or viability from the control group.

Changes in rBMSC cytoskeleton induced by copper treatment

After 5 days culture, the 4 groups of rBMSCs (Control, Cu group, Osteo group, Osteo+Cu group) were observed by bright field microscopy (Fig. 2a–d). Cells were stained with fluorescent phalloidin, which is specific for cell F-actin. After culturing in growth medium, cells from the control group exhibited characteristic fibroblast-like phenotype with parallel actin stress fibres extending across the entire cytoplasm (Fig. 2e). Those from Cu group (Fig. 2f) had almost the same phenotype. After 5 days culture under osteogenic conditions, stress fibres of cells from the Osteo group became denser and had criss-cross patterning (Fig. 2g). In contrast, in those from the Osteo+Cu group, cell actin had was of similar phenotype to that of the control group (Fig. 2h).

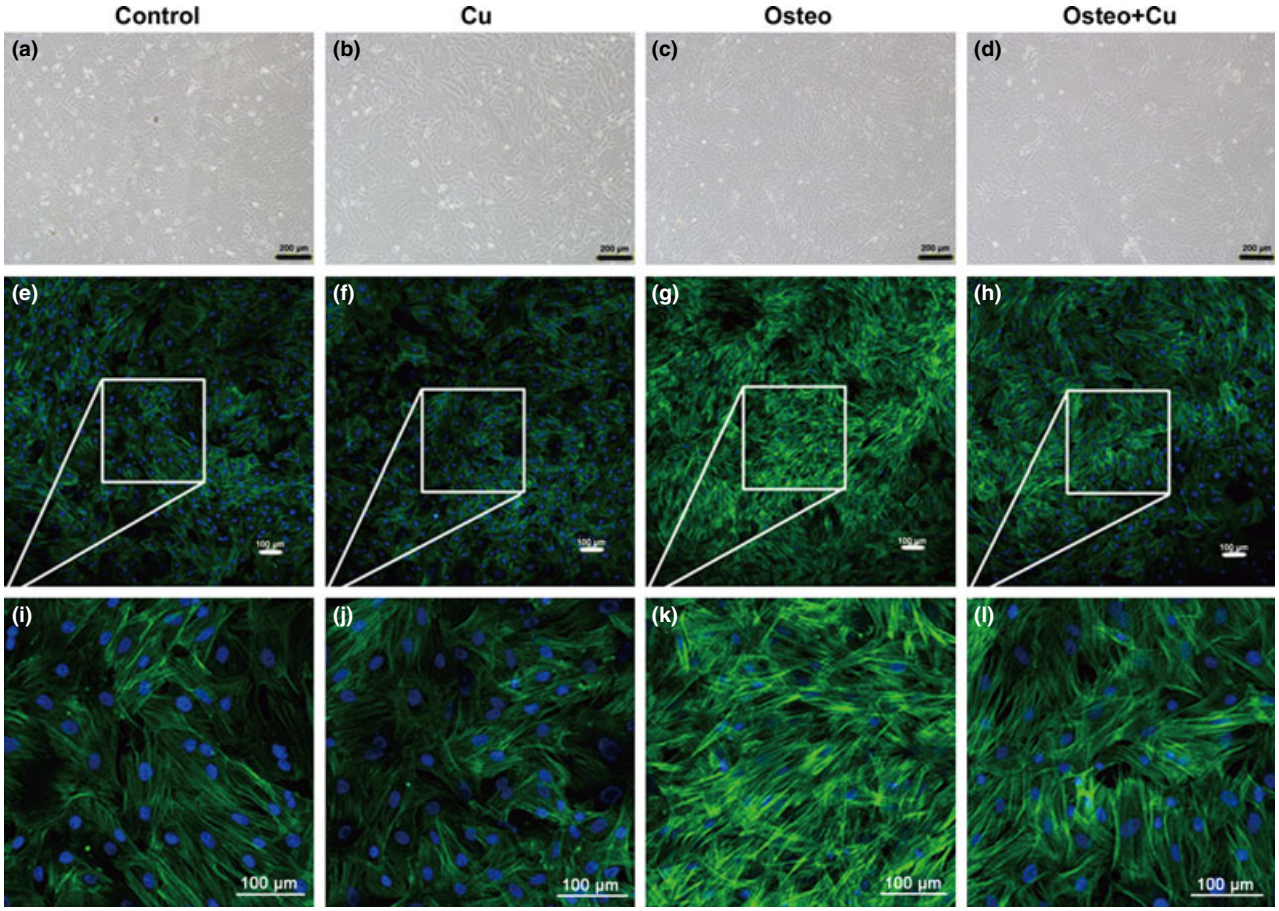

Figure 2. Cytoskeletal changes of rat bone marrow mesenchymal stem cells in each group. Control group (a), Cu group (b), Osteo group (c) and Osteo+Cu group (d) were observed under an inverted phase-contrast microscope. Scale bars represent 200 μm, original magnification: ×100. Representative images of fluorescently stained actin cytoskeleton of the Control group (e), Cu group (f), Osteo group (g), Osteo+Cu group (h). Scale bars represent 100 μm, original magnification: ×100. i ~l are amplified images. Cells were stained with fluorescent phalloidin, which is specific for cellular F-actin.

Inhibition of osteogenic differentiation of rBMSCs by copper

To assess effects of copper on osteogenic differentiation of rBMSCs, ALP staining was employed to assess extent of osteogenic differentiation. After 7 days osteogenic-induced differentiation, few ALP activity-positive red cells were found in either control or copper-treated groups (Fig. 3c,d); in contrast, many positive-stained cells were observed in the Osteo group (Fig. 3e); in the Osteo+Cu group, fewer such cells were found (Fig. 3f). After 3 weeks osteogenic differentiation, bone nodules became noticeable only in the Osteo group (Fig. 3i), but not in control, copper-treated and Osteo+Cu groups (Fig. 3g,h,j). By alizarin red S staining, no bone nodules were found in controls, copper-treated and Osteo+Cu groups (Fig. 3k,l,n). In contrast, abundant bone nodules were found in the Osteo group (Fig. 3m).

Inhibition of osteogenesis-related gene expression and down-regulation of Runx2 pathway by copper

Q-PCR was employed to analyse changes in gene expression after 7 days osteogenic differentiation (Fig. 4a). As discovered, normalized expressions of *Runx2*, *OSX*, *ALP*, *BMP2*, *OCN*, *OPN*, *ColIII* and *ColI* in the Osteo+Cu group were 145.1 ± 4.0%, 229.0 ± 10.6%, 111.1 ± 3.8%, 1756.6 ± 3.4%, 2481.7 ± 3.4%, 521.6 ± 16.2%, 586.9 ± 12.2% and 562.6 ± 10.9%, respectively, which were significantly lower than those of the Osteo group (230.3 ± 17.9%, 281.8 ± 25.6%, 137.2 ± 13.6%, 3143.7 ± 19.7%, 4973.2 ± 20.0%, 2105.7 ± 2.8%, 715.3 ± 17.9%, and 1030.0 ± 8.2%, respectively, $P < 0.05$ for all), suggesting that expression of osteogenic differentiation-related genes had been downregulated by copper. In the Osteo+Cu group, expression of *PPARγ2* (68.6 ± 4.0%) and *TWIST* (155.0 ± 5.8%) were higher compared

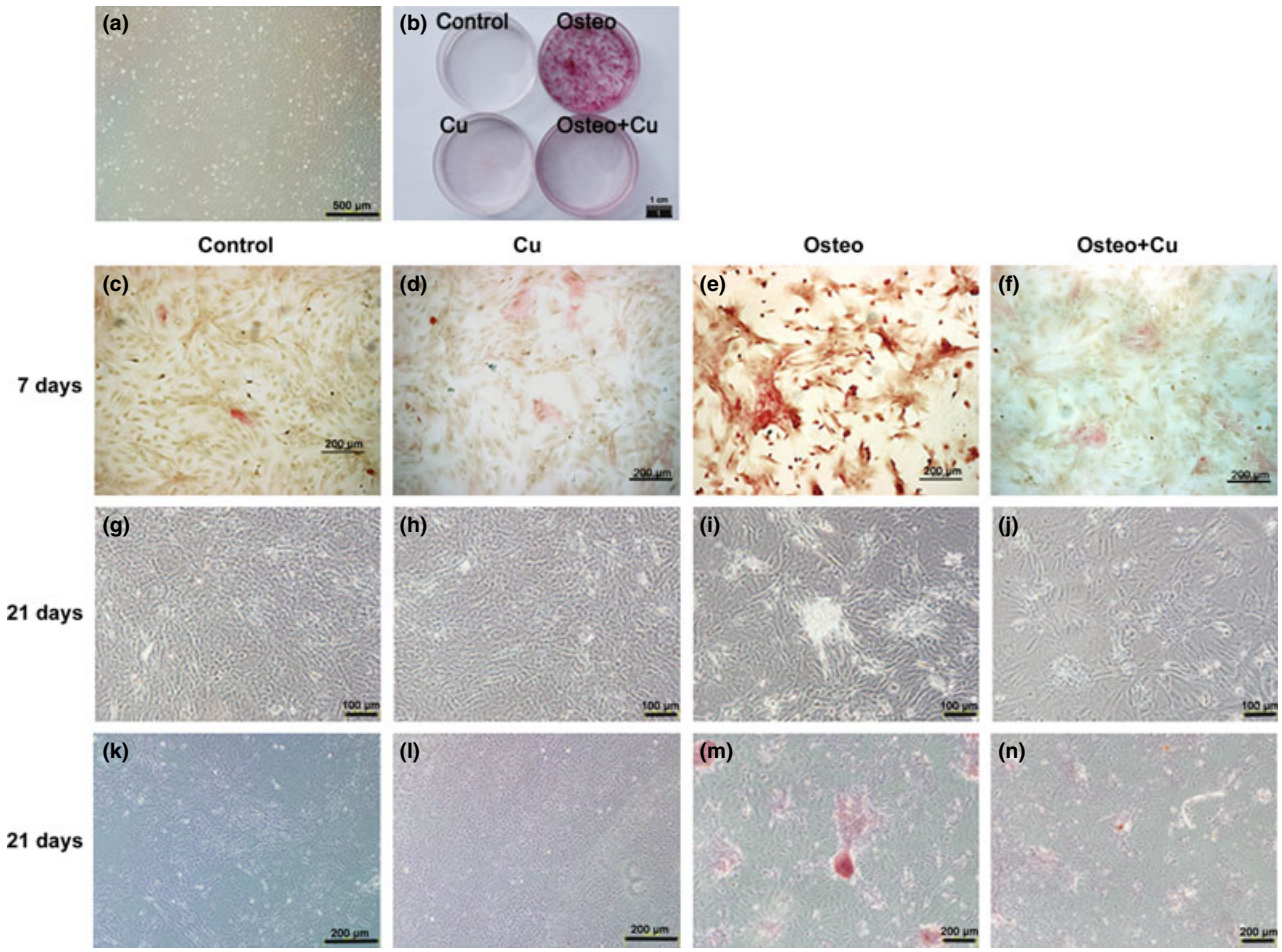

Figure 3. Effect of Cu on alkaline phosphatase (ALP) expression and matrix mineralization of osteogenic differentiated rat bone marrow mesenchymal stem cells (rBMSCs). rBMSCs from the third passage under a bright field microscope (a). Scale bars represent 500 μm, original magnification: ×40. General view of Alizarin red S staining (b) rBMSCs differentiation as induced by an osteogenic differentiation inducing medium supplemented with 5 μmol/l $CuSO_4$ for 7 days. Scale bars represent 1 cm. Active ALP of the control group (c), Cu group (d), Osteo group (e) and Osteo+Cu group (f) were detected. Scale bars represent 200 μm, original magnification: ×100. After 21 days of culture, photos were taken under an inverted phase-contrast microscope for the control group (g), Cu group (h), Osteo group (i) and Osteo+Cu group (j). Scale bars represent 100 μm, original magnification: ×200. Matrix mineralization of the control group (k), Cu group (l), Osteo group (m) and Osteo+Cu group (n) were visualized by Alizarin red S staining. Scale bars represent 200 μm, original magnification: ×100.

to the Osteo group (49.0 ± 2.5% and 122.7 ± 15.4%). By western blotting, expression of HIF1-α was shown to be increased by 5 μM Cu supplementation (Fig. 4b). Expression of Runx2 and OCN in the Osteo+Cu group was lower than in the Osteo group (Fig. 4c). On the other hand, expression of PPARγ2 was significantly higher in the former group (Fig. 4c). To normalize data, *Gapdh* had been used as an internal reference for each reaction.

Inhibition of collagen accumulation by copper in the rat model of ectopic bone formation

Two weeks after implantation of DBM/ALG/rBMSCs material, multinucleate giant cells were found in proximity to implants in both control and Cu groups. As a sign of resorption, lacunae had started to form at implant surfaces (Fig. 5a,b). Two months after implantation, microvascular formation, collagen accumulation and fibre-like tissue formation were observed in both groups. As confirmed by H&E staining, implants had better potential for microvascular formation with copper supplementation (Fig. 5c,d). Masson's trichrome staining also showed that copper inhibited collagen accumulation around implants in the Cu group (Fig. 5e,f). By Sirius red staining, most of fibre-like tissues were comprised of collagen typeI (Fig. 5g,h).

Discussion

In the present study, we assessed effects and mechanisms of copper for suppressing osteogenic differentiation of

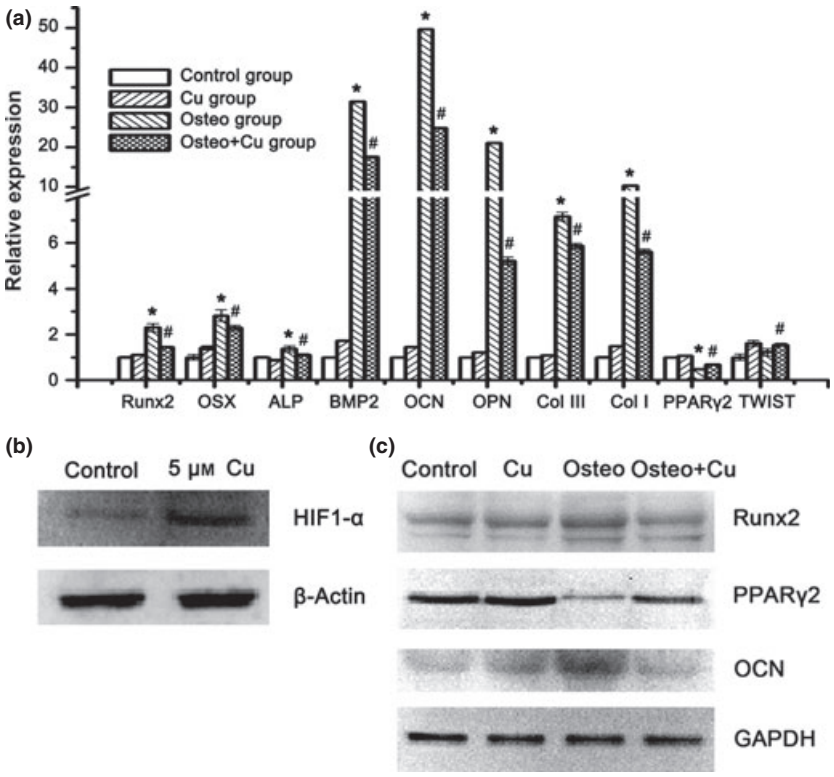

Figure 4. Analysis of osteogenic differentiation-related genes. (a) Expression of *Runx2*, *Osx*, *Alp*, *Bmp2*, *Ocn*, *Opn*, *Col III*, *Col I*, *Pparγ2* and *TWIST* genes as detected by Q-PCR after 7 days of culture. Each experiment consisted of triplicate samples for a treatment. Values are presented as mean ± SEM. *Significantly different from the Control group ($P < 0.05$). #Significantly different from the Osteo group ($P < 0.05$). (b) Protein expression of HIF1-α and β-actin as detected by Western blotting. (c) Expression of Gapdh, Runx2, Pparγ2 and Ocn proteins as detected by Western blotting.

rBMSCs cultured *in vitro*. Using a rat model for ectopic bone formation, we also demonstrated that copper could influence collagen accumulation and angiogenesis during *in vivo* bone formation. Our results suggest that copper may suppress osteogenic differentiation of MSCs and inhibit *in vivo* bone formation *via* the Runx2 signalling pathway. Expression of *Runx2* and other osteogenic differentiation-related genes could be downregulated by copper and the *in vivo* study also confirmed that copper could inhibit collagen formation whilst promoting angiogenesis.

Here, 5 μmol/l was used as final concentration of copper supplementation. To determine the physiological range of copper under the experimental conditions, MTT assay and cell viability testing were used to evaluate cell viability. We found that copper had no impact on viability of cells at below 10 μmol/l, but had cytotoxic effects when over 10 μmol/l. The safe concentration of 5 μmol/l for *in vitro* studies may be extrapolated to *in vivo* experimental conditions and used for animal studies.

As discovered, actin cytoskeleton of MSCs changed upon osteogenesis (25,26). At the beginning of osteogenic differentiation, MSCs had significant changes in both morphology and cytoskeleton. Fibroblast-like, spindle-shaped MSCs changed into long, thin stress fibres running parallel to orientation of the cells. However, upon osteogenic differentiation, parallel fibres gradually disappeared, while denser, criss-crossed patterning of actin cytoskeleton emerged, with stress fibres becoming thicker (25,26). In this study, we demonstrated that copper suppressed cytoskeletal changes of rBMSCs during osteogenic differentiation. After 5 days culture, the rBMSC actin fibres started to change from being parallel to being disordered with thicker stress fibres. However, with copper supplement alone, actin fibres remained parallel; this suggests that copper inhibited the MSC osteogenesis by interfering with cytoskeleton organization.

As demonstrated, copper suppressed osteogenic differentiation of rBMSCs. When the cells were cultured in osteogenic differentiation-inducing medium, they had lower expression of osteogenesis-related genes. Copper uptake in cells normally is mediated by a homotrimeric transporter CTR1 (27). When it is taken into the cytoplasm, chaperones such as the copper chaperone for superoxide dismutase 1 (CCS) start to deliver copper to specific targets. Copper is probably also required for binding of HIF-1 to hypoxia-responsive element sequence, which is CCS-dependent (28). Higher concentrations of copper stabilize HIF-1α, resulting in accumulation of HIF-1α, and enhanced HIF transcriptional activity (21,22). In the present study, expression of HIF-1α was upregulated at protein level when rBMSCs were

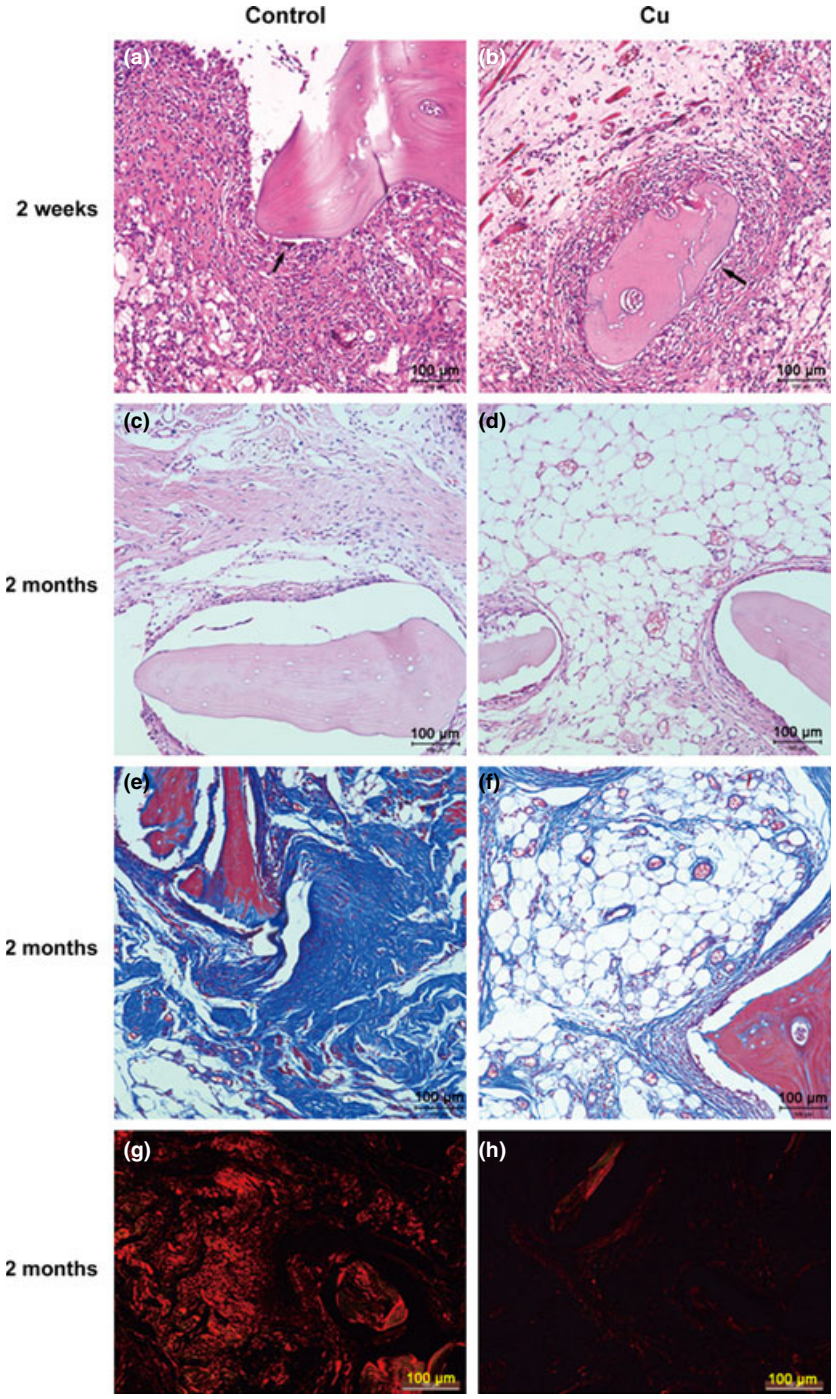

Figure 5. Representative images of histological analysis. H&E stain of the control and Cu groups at 2 weeks (a and b) and 2 months after the implantation (c and d). Masson stain at 2 months after the implantation in the control group (e) and Cu group (f). Representative histological analysis (Sirius red staining) at 2 months after the implantation in the control (g) and Cu groups (h). Scale bars represent 100 μm, original magnification: ×200.

cultured with 5 μM $CuSO_4$. As previously described, hypoxia can also inhibit osteogenesis by MSCs and osteoblasts (29), and Runx2 has been considered to be the main regulator of osteoblast phenotype. We have confirmed that copper can downregulate expression of Runx2 at both mRNA and protein levels. A further recent study has also indicated that hypoxia can inhibit osteogenic differentiation of MSCs through direct regulation of Runx2 by TWIST (23).Here, we also found *TWIST* mRNA level to be upregulated by copper supplementation. Thus, inhibition of osteogenic differentiation of MSCs by copper may have been through stabilization of HIF-1α and downregulation of *Runx2* expression. Furthermore, copper supplementation can also stimulate adipogenic differentiation of MSCs (30); it can also stimulate expression of *PPARγ2* at both mRNA and

protein levels, which seems to suggest that there is a balance between osteogenic and adipogenic differentiation. However, we did not find any differentiation of lipid droplet accumulation in adipogenic conditions with copper supplementation (Fig. S3). We propose that changes in mRNA level of *PPARγ2* might have been feedback for inhibited expression of osteogenesis-related genes. To keep stem cells in a relatively primitive state may enable better use of them. In the present study, we found that osteogenic differentiation of MSCs could be inhibited by copper supplementation. Whether this was been caused by delay in the cell cycle is worthy of further study.

By the *in vivo* bone formation experiment (31), we demonstrated that copper inhibited accumulation of collagen type I and fibre-like tissue formation whilst stimulating microvascular formation. Thus, there may be a balance between inhibition of collagen accumulation and promotion of microvascular formation with copper supplementation. Taken together, our findings can facilitate design of copper-containing implants for promoting angiogenesis. The ability of copper to suppress bone formation and stimulate angiogenesis may also lead to new applications in tissue engineering, which require angiogenesis and prevention of calcification, as in the cases of myocardial patches (32), blood vessels (33) and cartilage (34). For its dual role of promoting angiogenesis and suppressing osteogenesis, whether to use copper for bone tissue engineering (particularly for tumour patients) seems debatable. Safety issues must be taken into consideration when copper is used as a therapeutic agent to promote vascularization.

In conclusion, our study has demonstrated that copper can inhibit *in vitro* osteogenesis of rBMSCs and *in vivo* bone formation by suppressing the Runx2 signalling pathway, which in turn can suppress accumulation of collagen during the bone formation process. Further understanding of this may enable better application of copper for bone and other tissue engineering.

Acknowledgments

The authors thank Ms. Xiu-qun Li, Qun-ying Li and Lin Bai for their technical support. This work was jointly supported by the National Natural Science Foundation of China (31271058) and the National High Technology Research and Development Program of China (2012AA020503).

References

1 Haller A (1763) Experimentorum de ossiem formatione, in Opera minora. Lausanne: Francisci Grasset, 400pp.
2 Hunter J (1794) A Treatise on the Blood, Inflammation and Gunshot Wounds. London, UK: G Nichol.
3 Kanczler JM, Oreffo RO (2008) Osteogenesis and angiogenesis: the potential for engineering bone. *Eur. Cell Mater.* **2**, 100–114.
4 Portal-Núñez S, Lozano D, Esbrit P (2012) Role of angiogenesis on bone formation. *Histol. Histopathol.* **27**, 559–566.
5 Terpos E, Asli B, Christoulas D, Brouet JC, Kastritis E, Rybojad M *et al.* (2012) Increased angiogenesis and enhanced bone formation in patients with IgM monoclonal gammopathy and urticarial skin rash: new insight into the biology of Schnitzler syndrome. *Haematologica* **97**, 1699–1703.
6 Fang TD, Salim A, Xia W, Nacamuli RP, Guccione S, Song HM *et al.* (2005) Angiogenesis is required for successful bone induction during distraction osteogenesis. *J. Bone Miner. Res.* **20**, 1114–1124.
7 Hu GF (1998) Copper stimulates proliferation of human endothelial cells under culture. *J. Cell. Biochem.* **69**, 326–335.
8 Xie H, Kang YJ (2009) Role of copper in angiogenesis and its medicinal implications. *Curr. Med. Chem.* **16**, 1304–1314.
9 Giavaresi G, Torricelli P, Fornasari PM, Giardino R, Barbucci R, Leone G (2005) Blood vessel formation after soft-tissue implantation of hyaluronan-based hydrogel supplemented with copper ions. *Biomaterials* **26**, 3001–3008.
10 Gérard C, Bordeleau LJ, Barralet J, Doillon CJ (2010) The stimulation of angiogenesis and collagen deposition by copper. *Biomaterials* **31**, 824–831.
11 Will J, Melcher R, Treul C, Travitzky N, Kneser U, Polykandriotis E *et al.* (2008) Porous ceramic bone scaffolds for vascularized bone tissue regeneration. *J. Mater. Sci. Mater. Med.* **19**, 2781–2790.
12 Barralet J, Gbureck U, Habibovic P, Vorndran E, Gerard C, Doillon CJ (2009) Angiogenesis in calcium phosphate scaffolds by inorganic copper ion release. *Tissue Eng. Part A* **5**, 1601–1609.
13 Seong JM, Kim BC, Park JH, Kwon IK, Mantalaris A, Hwang YS (2010) Stem cells in bone tissue engineering. *Biomed. Mater.* **5**, 062001.
14 Drosse I, Volkmer E, Capanna R, De Biase P, Mutschler W, Schieker M (2008) Tissue engineering for bone defect healing: an update on a multi-component approach. *Injury* **39**(Suppl 2), S9–S20.
15 Rodríguez JP, Ríos S, González M (2002) Modulation of the proliferation and differentiation of human mesenchymal stem cells by copper. *J. Cell. Biochem.* **85**, 92–100.
16 Lüthen F, Bergemann C, Bulnheim U, Prinz C, Neumann HG, Podbielski A *et al.* (2010) A dual role of copper on the surface of bone implants. *Mater. Sci. Forum* **600**, 638–642.
17 Li S, Xie H, Li S, Kang YJ (2012) Copper stimulates growth of human umbilical vein endothelial cells in a vascular endothelial growth factor-independent pathway. *Exp. Biol. Med.* **237**, 77–82.
18 Jiang Y, Reynolds C, Xiao C, Feng W, Zhou Z, Rodriguez W *et al.* (2007) Dietary copper supplementation reverses hypertrophic cardiomyopathy induced by chronic pressure overload in mice. *J. Exp. Med.* **204**, 657–666.
19 Ducy P, Zhang R, Geoffroy V, Ridall AL, Karsenty G (1997) Osf2/Cbfa1: a transcriptional activator of osteoblast differentiation. *Cell* **89**, 747–754.
20 Komori T, Yagi H, Nomura S, Yamaguchi A, Sasaki K, Deguchi K *et al.* (1997) Targeted disruption of Cbfa1 results in a complete lack of bone formation owing to maturational arrest of osteoblasts. *Cell* **89**, 755–764.
21 Martin F, Linden T, Katschinski DM, Oehme F, Flamme I, Mukhopadhyay CK *et al.* (2005) Copper-dependent activation of hypoxia-inducible factor (HIF)-1: implications for ceruloplasmin regulation. *Blood* **105**, 4613–4619.

22 Li Q, Chen H, Huang X, Costa M (2006) Effects of 12 metal ions on iron regulatory protein 1 (IRP-1) and hypoxia-inducible factor-1 alpha (HIF-1alpha) and HIF-regulated genes. *Toxicol. Appl. Pharmacol.* **213**, 245–255.
23 Yang DC, Yang MH, Tsai CC, Huang TF, Chen YH, Hung SC (2011) Hypoxia inhibits osteogenesis in human mesenchymal stem cells through direct regulation of RUNX2 by TWIST. *PLoS One* **6**, e23965.
24 Huang YZ, Cai JQ, Xue J, Chen XH, Zhang CL, Li XQ *et al.* (2012) The poor osteoinductive capability of human acellular bone matrix. *Int. J. Artif. Organs* **35**, 1061–1069.
25 Yourek G, Hussain MA, Mao JJ (2007) Cytoskeletal changes of mesenchymal stem cells during differentiation. *ASAIO J.* **53**, 219–228.
26 Rodríguez JP, González M, Ríos S, Cambiazo V (2004) Cytoskeletal organization of human mesenchymal stem cells (MSC) changes during their osteogenic differentiation. *J. Cell. Biochem.* **93**, 721–731.
27 Zhou B, Gitschier J (1997) *hCTR1*: a human gene for copper uptake identified by complementation in yeast. *Proc. Natl. Acad. Sci. USA* **94**, 7481–7486.
28 Feng W, Ye F, Xue W, Zhou Z, Kang YJ (2009) Copper regulation of hypoxia-inducible factor-1 activity. *Mol. Pharmacol.* **75**, 174–182.
29 Potier E, Ferreira E, Andriamanalijaona R, Pujol JP, Oudina K, Logeart-Avramoglou D *et al.* (2007) Hypoxia affects mesenchymal stromal cell osteogenic differentiation and angiogenic factor expression. *Bone* **40**, 1078–1087.
30 Hoshiba T, Kawazoe N, Chen G (2012) The balance of osteogenic and adipogenic differentiation in human mesenchymal stem cells by matrices that mimic stepwise tissue development. *Biomaterials* **33**, 2025–2031.
31 Scott MA, Levi B, Askarinam A, Nguyen A, Rackohn T, Ting K *et al.* (2012) Brief review of models of ectopic bone formation. *Stem Cells Dev.* **21**, 655–667.
32 Rippel RA, Ghanbari H, Seifalian AM (2012) Tissue-engineered heart valve: future of cardiac surgery. *World J. Surg.* **36**, 1581–1591.
33 Karwowski W, Naumnik B, Szczepański M, Myśliwiec M (2012) The mechanism of vascular calcification – a systematic review. *Med. Sci. Monit.* **18**, 1–11.
34 Amizuka N, Hasegawa T, Oda K, Luiz de Freitas PH, Hoshi K, Li M *et al.* (2012) Histology of epiphyseal cartilage calcification and endochondral ossification. *Front. Biosci.* **4**, 2085–2100.

Supporting Information

Additional Supporting Information may be found in the online version of this article:

Table S1. Primer sequences for Q-PCR analysis.

Fig. S1. Ectopic bone formation test.

Fig. S2. Osteogenic, adipogenic and chondrogenic differentiation of rBMSCs.

Fig. S3. Effect of Cu on lipid droplet accumulation during adipogenic differentiation lipid droplets of Control group (a) and Cu group (b) were visualized by Oil red staining.